

# Some Fracture Mechanics Relationships for Thin Sheet Materials

A. M. SULLIVAN AND J. STOOP

*Strength of Metals Branch  
Metallurgy Division*

December 21, 1973



**NAVAL RESEARCH LABORATORY**  
**Washington, D.C.**

## CONTENTS

|  |     |
|--|-----|
| Abstract .....   | ii  |
| Symbols .....  | iii |
| INTRODUCTION .....   | 1   |
| EXPERIMENTAL PARAMETERS .....                                | 1   |
| Materials .....  | 1   |
| Test Procedure .....   | 1   |
| Data Analysis .....  | 3   |
| DEGRADATION OF $K_c$ WITH INCREASED<br>YIELD STRENGTH .....  | 6   |
| DEPENDENCE OF $K_c$ ON FRACTURE APPEARANCE ....              | 6   |
| RELATIONSHIP BETWEEN INITIAL AND FINAL<br>CRACK LENGTH ..... | 15  |
| SPECIMEN SCREENING .....                                     | 18  |
| CONCLUSIONS .....  | 18  |
| ACKNOWLEDGMENT .....   | 19  |
| REFERENCES .....   | 19  |

## ABSTRACT

The fracture resistance parameter  $K_c$  has been determined for a number of aluminum, titanium, and steel alloy sheet materials over a thickness range of 0.032 to 0.25 in. (0.8 to 6.25 mm). Several interesting  $K_c$  relationships have been developed from these investigations.

The  $K_c$  parameter is found to depend inversely upon the material yield stress. Further, a relationship can be established between  $K_c$  and fracture appearance. Analysis of the data has also disclosed that the amount of crack extension, i.e., final crack length  $2a_c$  appears to be influenced by the initial crack length. A straight-line curve in logarithmic coordinates relates the ratio of initial to final crack length,  $a_0/a_c$  to  $1/\beta_c$ ; this is justified by statistical analyses.

The development of these relationships can be of real assistance in the design of a standard initial screening test for  $K_c$ .

## PROBLEM STATUS

This is a final report on one phase of a continuing NRL problem.

## AUTHORIZATION

NRL Problem M01-24  
Project RR 022-01-46-5431

Manuscript submitted August 27, 1973.

## SYMBOLS

|  |   |
|--|---|
| $2a, 2a_0, 2a_c$                               | Crack or notch length in sheet; subscripts 0 and $c$ refer respectively to initial and critical values  |
| $r_y$  | Plastic zone size   |
| $r_{xy}$                                       | Correlation coefficient   |
| $A$  | Cross-sectional area of specimen, $BW$  |
| $B$  | Specimen thickness  |
| $B_F$  | Amount of flat fracture   |
| $B_{SL}$                                       | Amount of slant (or shear) fracture   |
| $CCT$  | Center-cracked tension specimen   |
| $E$  | Young's modulus   |
| $F$  | Statistical distribution  |
| $K, K_c, K_{Ic}$                               | Fracture resistance parameter; subscripts $c$ and $Ic$ refer to critical values under conditions of plane stress and plane strain, respectively |
| $P$  | Load  |
| $W$  | Specimen width  |
| $\mathcal{J}, \mathcal{J}_c, \mathcal{J}_{Ic}$ | Crack extension force; subscripts $c$ and $Ic$ refer to critical values under conditions of plane stress and plane strain, respectively         |
| $\beta_c$                                      | $\frac{1}{B} \left( \frac{K_c}{\sigma_{ys}} \right)^2$  |
| $\sigma_G$                                     | Gross or nominal stress, $P/A$  |
| $\sigma_{ys}$                                  | Yield stress  |

## SOME FRACTURE MECHANICS RELATIONSHIPS FOR THIN SHEET MATERIALS

### INTRODUCTION

The parallel demands of today's structural engineers for high strength and light weight in thin sheet materials imposes the obligation of insuring against catastrophic fracture by considering the fracture resistant properties of such materials. Fracture resistance can be defined as the ability of a material to withstand the deleterious effects of cracks, flaws, or notches while under load. One measurement of fracture resistance in thin sheet materials is the plane-stress fracture mechanics parameter  $K_c$ . Unlike other mechanical properties, however, the accurate determination of  $K_c$  is a function of  $K_c$  itself, since specimen size depends upon the ratio of  $K_c$  to yield stress,  $K_c/\sigma_{ys}$ . Other geometrical factors involved are crack length-to-width ratio  $2a/W$  and material thickness  $B$ . These interconnected dependencies preclude the development of a single standard test specimen unless one is chosen so large as to be economically indefensible.

Since research conducted over the past three years at NRL has established guidelines to assist in the estimation of allowable specimen width and crack length-to-width ratio, it is appropriate to consider the relationships between  $K_c$ , yield strength, and fracture appearance. Further, since crack growth occurs under load in the  $K_c$  specimen, some analyses of crack growth characteristics seem advisable.

### EXPERIMENTAL PARAMETERS

#### Materials

The materials studied include eight aluminum, four titanium, and five steel alloys in sheet form with thicknesses ranging from 0.032 to 0.25 in. (0.8 to 6.25 mm). Full details of the mechanical and fracture resistance properties are available (1-13). Relevant data are presented in Tables 1-4. In all specimens the fracture path was parallel to the rolling direction of the sheet ( $TL$ ).

#### Test Procedure

The center cracked tensile (CCT) specimen was utilized for the determination of  $K_c$ . Crack opening is measured by a strain-gage-instrumented displacement probe positioned in a circular hole in the center of the initial slit. This displacement measurement (COD) is referred to a normalized experimental calibration curve which relates the amount of crack opening to the instantaneous crack length of the specimen. Both load and COD are simultaneously graphed by an x-y recorder until failure occurs. These techniques have been previously discussed (1,5). Values of slant fracture percent were calculated from measurements made by a micrometer slide comparator at three positions ahead of the critical crack.

Table 1  
Fracture Resistance Data for Aluminum Alloys

| Alloy                | $B$<br>(in.) | $W$<br>(in.) | $2a_0$<br>(in.) | $2a_c$<br>(in.) | $\sigma_{ys}$<br>(ksi) | $K_c$<br>(ksi $\sqrt{\text{in.}}$ ) | Percent<br>Slant | $\beta_c^\ddagger$ |
|----------------------|--------------|--------------|-----------------|-----------------|------------------------|-------------------------------------|------------------|--------------------|
| 7178-T6              | 0.040        | 12           | 2.130           | 2.40            | 79                     | 49                                  | 53               | 9.7                |
|                      | 0.063        | 12           | 2.124           | 2.40            | 78                     | 50                                  | 50               | 6.4                |
|                      | 0.091        | 12           | 2.138           | 2.40            | 78                     | 44                                  | 50               | 3.6                |
|                      | 0.127        | 12           | 2.140           | 2.54            | 77                     | 45                                  | 44               | 2.7                |
|                      |              |              |                 |                 |                        |                                     |                  |                    |
| 7075-T6              | 0.032        | 12           | 2.130           | 2.54            | 71                     | 52                                  | 100              | 16.4               |
|                      | 0.063        | 12           | 2.220           | 2.23            | 76                     | 60                                  | —                | —                  |
|                      | 0.063        | 12           | 2.20            | 2.52            | —                      | 58                                  | —                | —                  |
|                      | 0.063        | 12           | 4.14            | 4.50            | —                      | 63                                  | —                | —                  |
|                      | 0.063        | 12           | 4.23            | 4.56            | —                      | 62                                  | 61               | 10.1               |
|                      | 0.093        | 12           | 2.094           | 2.46            | 74                     | 65                                  | 65               | 8.2                |
|                      | 0.102        | 12           | 2.154           | 2.56            | 75                     | 62                                  | 61               | 6.8                |
|                      | 0.126        | 12           | 2.116           | 3.04            | 76                     | 55                                  | 56               | 4.1                |
|                      | 0.198        | 12           | 2.098           | 3.26            | 76                     | 56                                  | 46               | 2.8                |
|                      | 0.250        | 12           | 2.130           | 2.70            | 74                     | 46                                  | 45               | 1.6                |
|                      |              |              |                 |                 |                        |                                     |                  |                    |
| 7079-T6              | 0.037        | 12           | 2.138           | 3.66            | 68                     | 62                                  | 84               | 21.9               |
|                      | 0.063        | 12           | 2.138           | 3.42            | 71                     | 71                                  | 79               | 15.7               |
|                      | 0.101        | 12           | 2.128           | 3.90            | 62                     | 98                                  | 78               | 24.9               |
|                      | 0.140        | 12           | 2.144           | 3.12            | 72                     | 68                                  | 48               | 6.5                |
|                      | 0.250        | 12           | 2.086           | 3.34            | 66                     | 81                                  | 41               | 6.0                |
| 2014-T6              | 0.040        | 12           | 2.156           | 3.18            | 62                     | 75                                  | 100              | 37.4               |
|                      | 0.063        | 12           | 2.120           | 3.06            | 61                     | 72                                  | 100              | 22.0               |
|                      | 0.091        | 12           | 2.129           | 3.10            | 57                     | 75                                  | 91               | 19.1               |
|                      | 0.125        | 12           | 2.100           | 3.80            | 60                     | 92                                  | 100              | 19.1               |
|                      | 0.250        | 12           | 2.118           | 3.20            | 59                     | 66                                  | 89               | 4.9                |
| 2219-T87             | 0.032        | 12           | 2.150           | 3.81            | 52                     | 86                                  | 100              | 84.4               |
|                      | 0.062        | 12           | 2.155           | 3.44            | 54                     | 77                                  | 100              | 32.9               |
|                      | 0.091        | 12           | 2.137           | 3.76            | 51                     | 92                                  | 100              | 35.6               |
|                      | 0.125        | 12           | 2.139           | 4.59            | 52                     | 88                                  | 100              | 22.8               |
|                      | 0.250        | 12           | 2.120           | 3.60            | 54                     | 76                                  | 100              | 8.0                |
| 7178-T6 <sup>†</sup> | 0.063        | 12           | 2.132           | 2.576           | 78                     | 36                                  | 42               | 3.5                |
|                      | 0.091        | 12           | 2.190           | 2.784           | 76                     | 45                                  | 32               | 3.9                |
|                      | 0.125        | 12           | 2.145           | 3.28            | 78                     | 48                                  | 34               | 2.9                |
|                      | 0.25         | 12           | 2.16            | 2.16            | 78                     | 36                                  | 23               | 0.84               |
|                      | 0.30         | 12           | 2.135           | 2.88            | 79                     | 36                                  | 17               | 0.71               |
| 7075-T6 <sup>†</sup> | 0.063        | 12           | 2.132           | 2.64            | 72                     | 70                                  | 44               | 14.8               |
|                      | 0.092        | 12           | 2.150           | 3.136           | 76                     | 77                                  | 50               | 11.5               |
|                      | 0.124        | 12           | 2.132           | 2.96            | 74                     | 61                                  | 38               | 5.4                |
|                      | 0.25         | 12           | 2.168           | 2.168           | 76                     | 42                                  | 25               | 1.2                |
|                      | 0.30         | 12           | 2.132           | 2.85            | 74                     | 46                                  | 21               | 1.3                |

<sup>†</sup> Rolled down from 0.30-in. sheet.

$$\ddagger\beta_c = \frac{1}{B}(K_c/\sigma_{ys})^2.$$

Table 2  
Fracture Resistance Data for Titanium Alloys

| Alloy       | $B$<br>(in.) | $W$<br>(in.) | $2a_0$<br>(in.) | $2a_c$<br>(in.) | $\sigma_{ys}$<br>(ksi) | $K_c$<br>(ksi $\sqrt{\text{in.}}$ ) | Percent<br>Slant | $\beta_c^\dagger$ |
|-------------|--------------|--------------|-----------------|-----------------|------------------------|-------------------------------------|------------------|-------------------|
| 6A1-4V      | 0.032        | 12           | 2.138           | 2.82            | 151                    | 54                                  | 100              | 4.00              |
|             | 0.062        | 12           | 2.132           | 2.70            | 158                    | 64                                  | 100              | 2.86              |
|             | 0.090        | 12           | 2.132           | 2.40            | 146                    | 77                                  | 100              | 2.66              |
| 4A1-3Mo-1V  | 0.042        | 12           | 2.144           | 2.144           | 162                    | 50                                  | 68               | 2.30              |
|             | 0.058        | 12           | 2.234           | 2.234           | 153                    | 54                                  | 59               | 2.30              |
|             | 0.087        | 12           | 2.290           | 2.290           | 152                    | 62                                  | 54               | 1.90              |
|             | 0.124        | 12           | 2.132           | 2.132           | 160                    | 35                                  | 46               | .38               |
| 16V-2.5A1   | 0.041        | 12           | 2.128           | 2.52            | 182                    | 52                                  | 100              | 2.00              |
|             | 0.059        | 12           | 2.137           | 2.137           | 176                    | 46                                  | 52               | 1.16              |
|             | 0.118        | 12           | 2.138           | 2.64            | 182                    | 44                                  | 53               | .51               |
| 13V-11A-3A1 | 0.040        | 12           | 2.152           | 2.152           | 198                    | 34                                  | 23               | .74               |
|             | 0.063        | 12           | 2.113           | 2.113           | 207                    | 38                                  | 26               | .56               |
|             | 0.091        | 12           | 2.116           | 2.116           | 201                    | 30                                  | 12               | .24               |
|             | 0.125        | 12           |                 |                 |                        |                                     | 11               | .09               |

$$\dagger \beta_c = \frac{1}{B} (K_c / \sigma_{ys})^2$$

### Data Analysis

Fracture resistance  $K_c$  is calculated according to equation (Ref. 14)

$$K_c = \sigma_G \sqrt{a_c} f(2a/W), \quad (1)$$

where

$$f(2a/W) = 1.77 \left[ \left( 1 - 0.1 \left( \frac{2a}{W} \right) + \left( \frac{2a}{W} \right)^2 \right) \right]. \quad (2)$$

Values of  $\sigma_G$  and  $2a_c$  are determined from the load and COD measurements mentioned above.

Regression lines, correlation coefficients and  $t$  and  $F$  statistical calculations were computed from conventional statistical definitions and equations (15,16).

### DEGRADATION OF $K_c$ WITH INCREASED YIELD STRENGTH

The fact that materials show a degradation in resistance to fracture  $K_{Ic}$  with increasing yield stress has long been recognized for thick plate material. As can be seen in Fig. 1, the same inverse relationship also exists for thin sheet alloys. Upper and lower limit lines define the highest and lowest  $K_c$  values measured with respect to yield strength for the alloy systems of aluminum, titanium, and steel. (Thicknesses from 0.032 to 0.25 in. are included.) The ratio lines  $K_c/\sigma_{ys}$  are accompanied by estimates of the minimum width requirement for the CCT specimen. Normalizing the data shown in Fig. 1 by the yield

Table 3  
Fracture Resistance Data for Steels

| Steel   | $B$<br>(in.) | $W$<br>(in.) | $2a_0^+$<br>(in.) | $2a_c^\dagger$<br>(in.) | $\sigma_{ys}$<br>(ksi) | $K_c$<br>(ksi $\sqrt{\text{in.}}$ ) | Percent<br>Slant | $\beta_c^\ddagger \S_{c \text{ ave}}$ |
|---------|--------------|--------------|-------------------|-------------------------|------------------------|-------------------------------------|------------------|---------------------------------------|
| 4130    | 0.032        | 12           | 2.18              | 4.00                    | 168                    | 151                                 | 100              | 21.80                                 |
|         | 0.032        | 12           | 4.51              | 6.84                    | 168                    | 146                                 | 100              |                                       |
|         | 0.050        | 12           | 2.21              | 4.56                    | 172                    | 172                                 | 100              | 20.10                                 |
|         | 0.050        | 12           | 4.17              | 6.72                    | 172                    | 174                                 | 100              |                                       |
|         | 0.063        | 12           | 2.26              | 3.78                    | 170                    | 172                                 | 100              | 18.20                                 |
|         | 0.063        | 12           | 4.21              | 6.54                    | 170                    | 191                                 | 100              |                                       |
|         | 0.087        | 12           | 2.20              | 3.26                    | 183                    | 124                                 | 78               | 4.85                                  |
|         | 0.087        | 12           | 4.18              | 6.07                    | 183                    | 144                                 | 84               | 4.85                                  |
|         | 0.125        | 12           | 2.21              | 3.54                    | 176                    | 148                                 | 91               | 6.80                                  |
|         | 0.125        | 12           | 4.18              | 5.86                    | 176                    | 158                                 | 92               |                                       |
| 4130    | 0.032        | 12           | 2.13              | 4.98                    | 185                    | 154                                 | 100              | 22.6                                  |
|         | 0.032        | 12           | 4.15              | 6.66                    | 185                    | 161                                 | 100              |                                       |
|         | 0.051        | 12           | 2.15              | 3.16                    | 185                    | 146                                 | 100              | 13.60                                 |
|         | 0.051        | 12           | 4.10              | 6.60                    | 185                    | 158                                 | 100              |                                       |
|         | 0.063        | 12           | 2.16              | 3.72                    | 178                    | 129                                 | 83               | 9.40                                  |
|         | 0.063        | 12           | 4.25              | 6.12                    | 178                    | 146                                 | —                |                                       |
|         | 0.087        | 12           | 2.10              | 3.26                    | 200                    | 123                                 | —                | 4.50                                  |
|         | 0.087        | 12           | 4.08              | 6.46                    | 200                    | 127                                 | 71               |                                       |
|         | 0.125        | 12           | 2.10              | 3.72                    | 191                    | 155                                 | —                | 4.60                                  |
|         | 0.125        | 12           | 4.10              | 4.92                    | 191                    | 138                                 | 77               |                                       |
|         | 0.250        | 12           | 2.20              | 4.22                    | 185                    | 163                                 | —                | 2.30                                  |
|         | 0.250        | 12           | 4.16              | 5.40                    | 185                    | 121                                 | 20               |                                       |
| D6A     | 0.098        | 12           | 2.10              | 2.10                    | 228                    | 54                                  | 21               | 0.66                                  |
|         | 0.098        | 12           | 4.09              | 4.09                    | 228                    | 62                                  | 20               |                                       |
|         | 0.190        | 12           | 2.12              | 2.12                    | 220                    | 48                                  | 10               | 0.23                                  |
|         | 0.190        | 12           | 4.12              | 4.12                    | 220                    | 45                                  | 9                |                                       |
|         | 0.25         | 12           | 2.16              | 2.16                    | 230                    | 68                                  | 14               | 0.45                                  |
|         | 0.25         | 12           | 4.14              | 4.14                    | 230                    | 86                                  | 16               |                                       |
| RSM-250 | 0.063        | 12           | 2.162             | 2.68                    | 244                    | 180                                 | 100              | 10.0                                  |
|         | 0.063        | 12           | 4.154             | 5.94                    | 244                    | 207                                 | 100              |                                       |
|         | 0.090        | 12           | 2.226             | 2.94                    | 246                    | 204                                 | 100              | 7.6                                   |
|         | 0.090        | 12           | 4.120             | 4.75                    | 246                    | 204                                 | 100              |                                       |
|         | 0.140        | 12           | 2.126             | 3.04                    | 248                    | 194                                 | 100              | 4.2                                   |
|         | 0.140        | 12           | 4.154             | 5.04                    | 248                    | 186                                 | 100              |                                       |

<sup>+</sup>Average values of  $a_0/a_c$  at each thickness were used for statistics.

<sup>†</sup>Average value of  $K_c$  at each thickness was used for  $\beta$  calculation.

$$\S_{\beta_c} = \frac{1}{B}(K_c/\sigma_{ys})^2.$$



Table 4  
Fracture Resistance Data for Aluminum 7475-T61

| $B$<br>(in.) | $W$<br>(in.) | $2a_0$<br>(in.) | $2a_c$<br>(in.) | $\sigma_{ys}$<br>(ksi) | $K_c$<br>(ksi $\sqrt{\text{in.}}$ ) | $\beta_c^\ddagger$ | $2a_c^\S$<br>(in.) | $K_c^\#$<br>(ksi $\sqrt{\text{in.}}$ ) | Percent<br>Difference |
|--------------|--------------|-----------------|-----------------|------------------------|-------------------------------------|--------------------|--------------------|--|-----------------------|
| 0.063        | 12           | 2.13            | 3.96            | 68                     | 123 <sup>†</sup>                    | 52.8               | 3.62               | 116                                    | -5.7                  |
| 0.063        | 12           | 3.13            | 5.04            | 68                     | 124 <sup>†</sup>                    | 52.8               | 5.32               | 128                                    | +3.2                  |
| 0.107        | 12           | 2.12            | 3.07            | 72                     | 103                                 | 19.1               | 3.26               | 106                                    | +2.9                  |
| 0.107        | 12           | 3.10            | 4.14            | 72                     | 105                                 | 19.9               | 4.78               | 117                                    | +11.4                 |
| 0.190        | 12           | 2.16            | 2.94            | 72                     | 102                                 | 9.0                | 3.06               | 105                                    | +2.9                  |
| 0.190        | 12           | 3.09            | 4.14            | 72                     | 87                                  | 7.6                | 4.30               | 90                                     | +3.4                  |
| 0.25         | 12           | 2.13            | 3.26            | 72                     | 96                                  | 7.0                | 2.94               | 91                                     | -5.2                  |
| 0.25         | 12           | 3.07            | 4.24            | 72                     | 102                                 | 8.0                | 4.28               | 104                                    | +2.0                  |
| 0.063        | 20           | 3.61            | 5.56            | 68                     | 130                                 | 60.6               | 5.20               | 120                                    | -7.7                  |
| 0.063        | 20           | 5.10            | 6.60            | 68                     | 111                                 | 42.4               | 8.48               | 132                                    | +18.9                 |
| 0.109        | 20           | 3.62            | 4.70            | 72                     | 107                                 | 20.4               | 5.60               | 118                                    | +10.2                 |
| 0.109        | 20           | 5.10            | 6.90            | 72                     | 108                                 | 20.8               | 7.88               | 118                                    | +9.2                  |
| 0.190        | 20           | 3.60            | 4.20            | 72                     | 80                                  | 6.4                | 4.92               | 88                                     | +10.0                 |
| 0.190        | 20           | 5.13            | 5.60            | 72                     | 76                                  | 5.8                | 6.96               | 88                                     | +15.8                 |
| 0.25         | 20           | 3.62            | 4.50            | 72                     | 88                                  | 5.9                | 4.92               | 93                                     | +5.6                  |
| 0.25         | 20           | 5.11            | 6.64            | 72                     | 99                                  | 7.4                | 7.10               | 104                                    | +5.0                  |

<sup>†</sup> $\sigma_{\text{net}} > \sigma_{ys}$

<sup>‡</sup> $\beta_c = \frac{1}{B} (K_c / \sigma_{ys})^2$

<sup>§</sup>Values calculated from Eq. (1).

<sup>#</sup>Values derived from calculated value of  $2a_c$ .

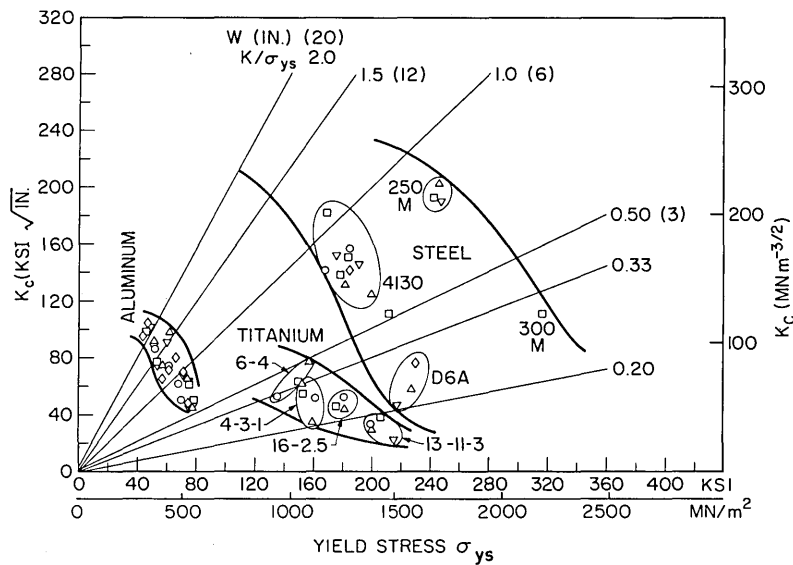


Fig. 1—Fracture resistance  $K_c$  vs yield stress  $\sigma_{ys}$ . Lines denote  $K_c/\sigma_{ys}$  ratio. An estimate of minimum specimen width  $W$  accompanies each ratio value

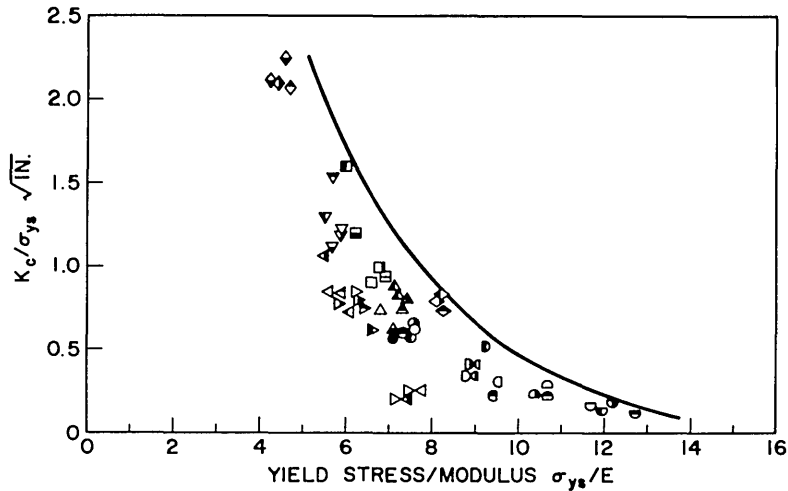


Fig. 2—Fracture resistance vs yield stress normalized as  $K_c/\sigma_{ys}$  vs  $\sigma_{ys}/E$

strength and elastic modulus gives the curve shown in Fig. 2. A similar curve could be plotted using yield stress and alloy density as normalizing factors.

These diagrams indicate the range of values observed. From them it is possible, knowing yield stress and modulus, to estimate an upper limit for the  $K_c$  of an unknown material so that an appropriate test specimen width can be selected. It can be noted that a "standard" width of 12 in. is sufficient for values of  $K/\sigma_{ys} \leq 1.5$ .

### DEPENDENCE OF $K_c$ ON FRACTURE APPEARANCE

Although attempts to describe the relationship of  $K_c$  and sheet thickness in terms of the two models proposed (17,18) have so far not proven satisfactory (6,7,10-12) it was noted and reported (6) that for titanium alloys there appeared to be some relationship between  $K_c$  and percent slant fracture within a wide scatterband. Reexamination of the data indicated that  $K_c$  values from test specimens containing both blunt and sharp notches had been incorporated in these initial plots. Accordingly, the data from three alloy systems were replotted using the sharp notch data only, with the results seen in Figs. 3a, 3b, 3c, and 3d.

However, inasmuch as slant or shear fracture indicates the involvement of an energy process, it seemed more reasonable to utilize the relationship  $K_c^2 = \mathcal{J}_c E$  and replot these data using the  $\mathcal{J}_c$  term. Figures 4a, 4b, 4c, and 4d disclose the unexpected result that the linear relationship between  $\mathcal{J}_c$  and percent slant appears to go through the origin. The schematic diagram of  $K$  vs crack growth seen in Fig. 5 indicates an increasing  $K$  value with no crack growth until an initiation value  $K_{Ic}$  is reached and thereafter, increasing values of  $K$  terminating in final  $K_c$  after some amount of crack growth. Since the  $K_{Ic}$  (or  $\mathcal{J}_{Ic}$ ) value is normally associated with a flat fracture appearance, that is, zero percent shear, it would have been reasonable to expect positive values of  $\mathcal{J}$  for each alloy at zero percent slant. However, since this was not the case, the slopes of the curves drawn were utilized to calculate  $\mathcal{J}_c$  from percent slant according to the following straight-line equations:

$$\text{Steel } \mathcal{J}_c = 740 \left( \frac{\text{in.-lb}}{\text{in.}^2} \right) \frac{B_{SL}}{B} \quad (3)$$

$$\text{Aluminum } \mathcal{J}_c = 550 \left( \frac{\text{in.-lb}}{\text{in.}^2} \right) \frac{B_{SL}}{B} \quad (4)$$

$$\text{Titanium } \mathcal{J}_c = 240 \left( \frac{\text{in.-lb}}{\text{in.}^2} \right) \frac{B_{SL}}{B}. \quad (5)$$

$\mathcal{J}_c$  was then converted to  $K_c$  values through the expression  $K = \sqrt{\mathcal{J}E}$ . The relationship between the calculated and measured values plotted in Fig. 6 was analyzed statistically. Although the regression curve  $K \text{ (calc.)} = 0.84 K \text{ (meas.)} + 5.24$  does not quite go through the origin, the correlation coefficient is high;  $r_{xy} = 0.92$ .

Considering that the so-called  $\mathcal{J}_c$  (or  $K_c$  value) is the total value, it was decided to analyze the data by subtracting  $\mathcal{J}_{Ic}$  values such that

$$\mathcal{J}_c^* = \mathcal{J}_c - \mathcal{J}_{Ic} \left( 1 - \frac{B_{SL}}{B} \right) \quad (6)$$

$$= \mathcal{J}_c - \mathcal{J}_{Ic} \left( \frac{B_F}{B} \right) \quad (7)$$

The  $\mathcal{J}_{Ic}$  values were estimated from the yield stress values of the materials utilizing relationships found in several NRL reports (19,20).

Figures 7a, 7b, and 7c show plots of these values against percent slant. Again, the curves appear to go through the origin and the same ordering of alloy systems persists, although the slopes are slightly altered to give the following set of straight-line equations:

$$\text{Steel } \mathcal{J}_c^* = 730 \left( \frac{\text{in.-lb}}{\text{in.}^2} \right) \frac{B_{SL}}{B} \quad (8)$$

$$\text{Aluminum } \mathcal{J}_c^* = 570 \left( \frac{\text{in.-lb}}{\text{in.}^2} \right) \frac{B_{SL}}{B} \quad (9)$$

$$\text{Titanium } \mathcal{J}_c^* = 195 \left( \frac{\text{in.-lb}}{\text{in.}^2} \right) \frac{B_{SL}}{B} \quad (10)$$

Regression analyses performed on these data for comparison with the drawn curves gave the following relationships:

$$\text{Steel } \mathcal{J}_c^* = 729 \left( \frac{\text{in.-lb}}{\text{in.}^2} \right) \frac{B_{SL}}{B} + 46 \left( \frac{\text{in.-lb}}{\text{in.}^2} \right) \quad (11)$$

$$\text{Aluminum } \mathcal{J}_c^* = 582 \left( \frac{\text{in.-lb}}{\text{in.}^2} \right) \frac{B_{SL}}{B} + 24 \left( \frac{\text{in.-lb}}{\text{in.}^2} \right) \quad (12)$$

$$\text{Titanium } \mathcal{J}_c^* = 192 \left( \frac{\text{in.-lb}}{\text{in.}^2} \right) \frac{B_{SL}}{B} + 6.6 \left( \frac{\text{in.-lb}}{\text{in.}^2} \right). \quad (13)$$

The correlation coefficient  $r_{xy}$  was also obtained for each alloy system; these values are

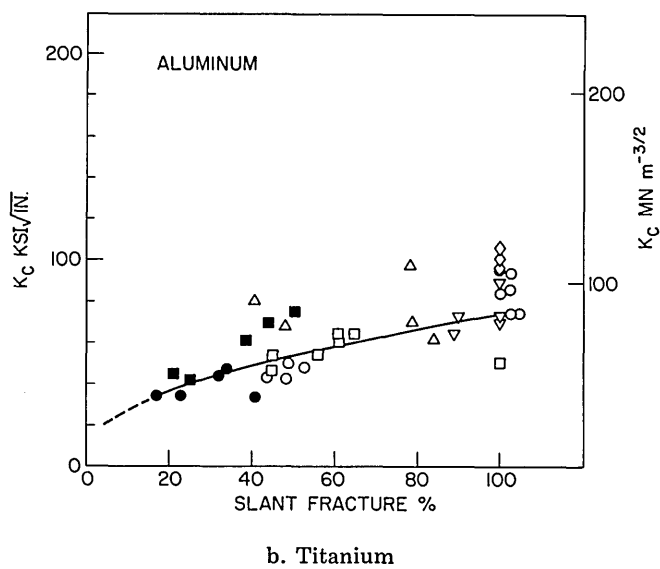
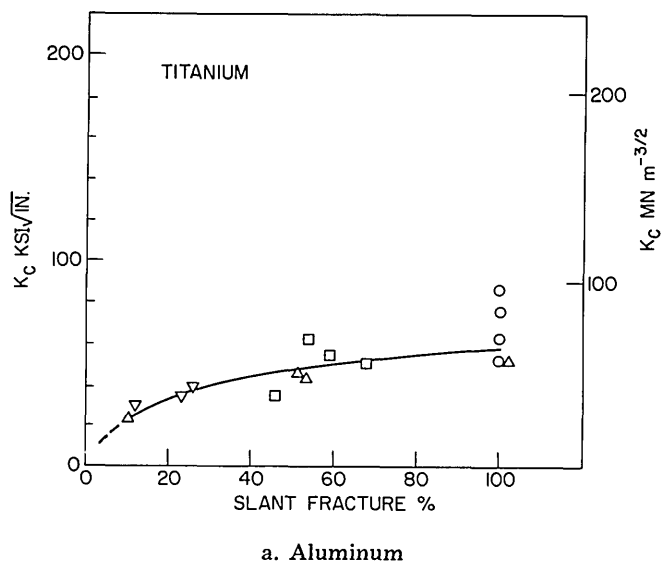
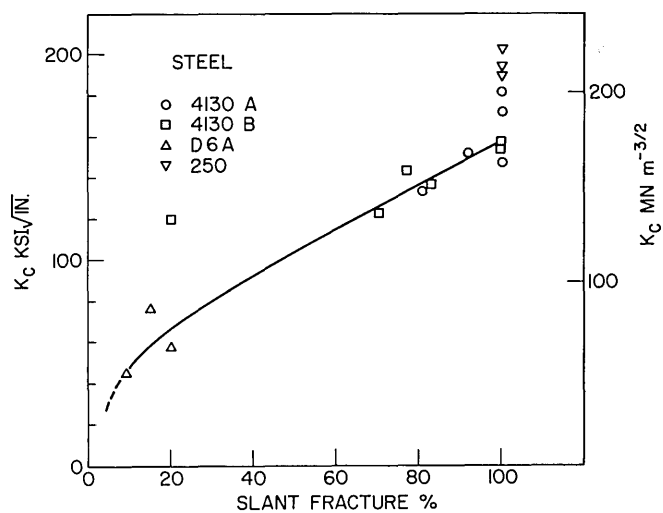
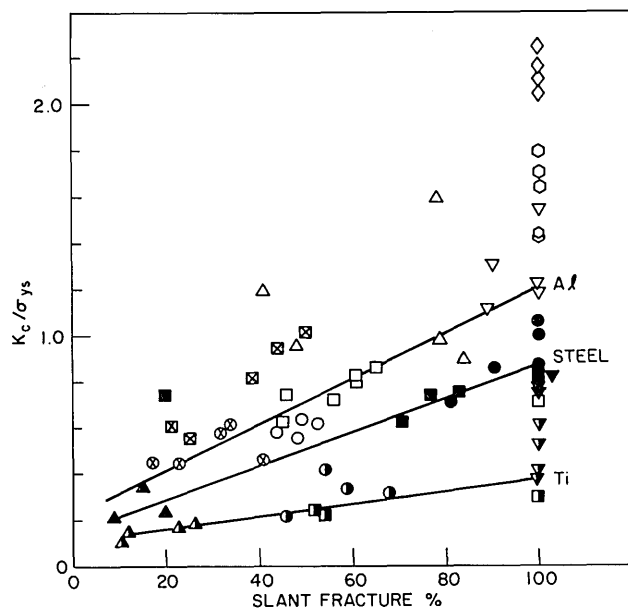
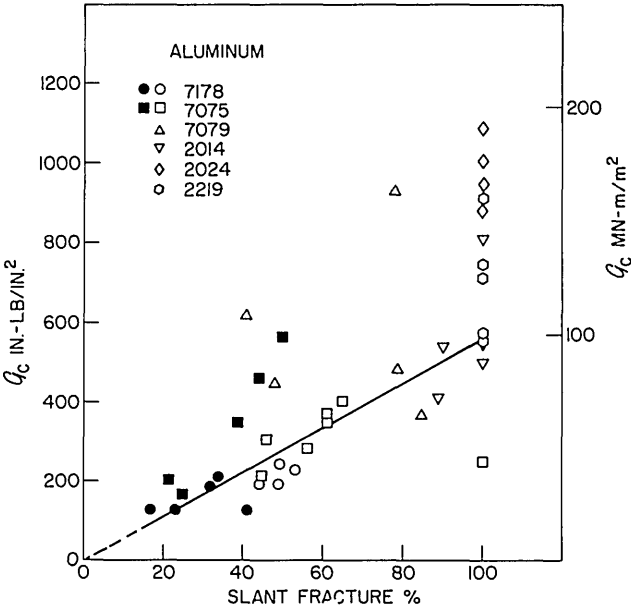


Fig. 3—Fracture resistance  $K_C$  vs percent slant fracture

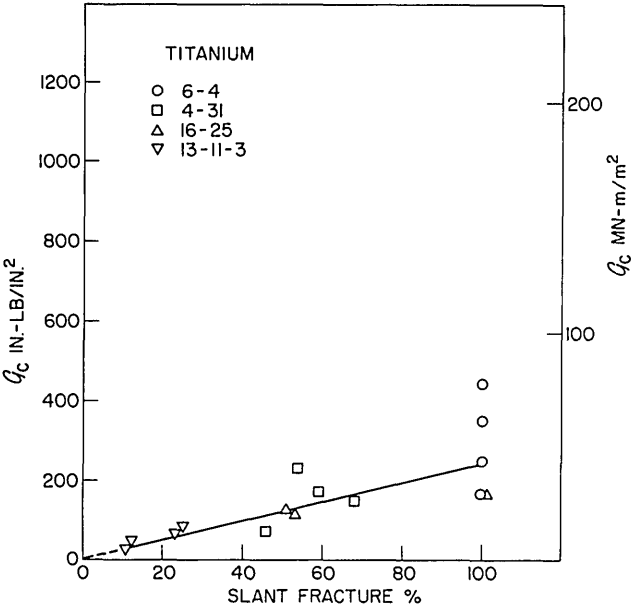


c. Steel

d. Normalized for all alloys as  $K_c/\sigma_{ys}$ Fig. 3 (Continued)—Fracture resistance  $K_c$  vs percent slant fracture

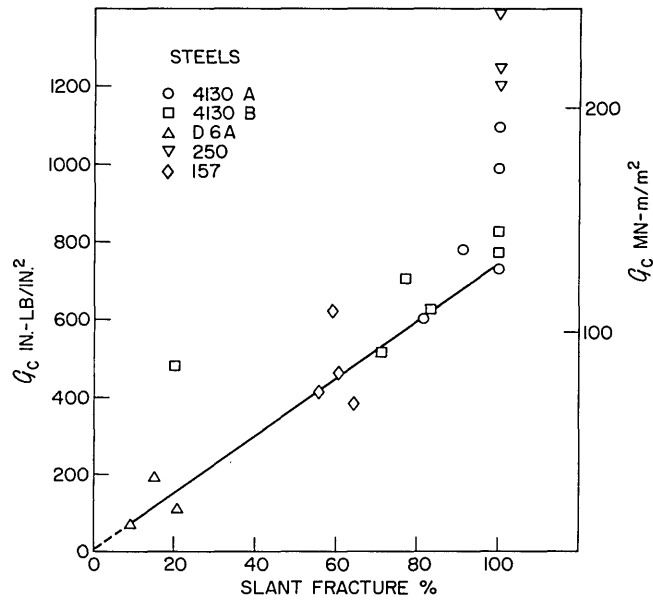


a. Aluminum

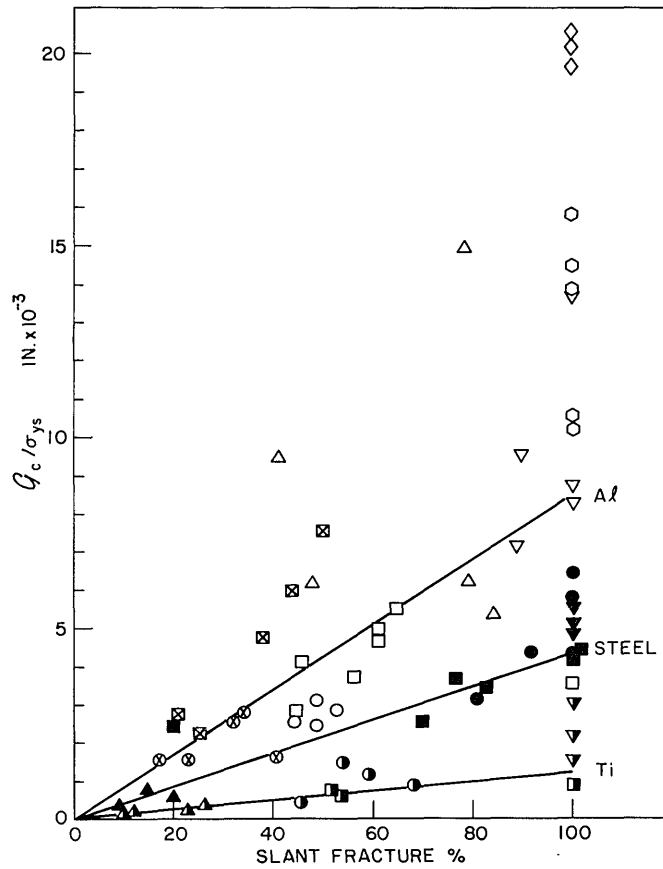


b. Titanium

Fig. 4—Crack extension force  $\mathcal{G}_c$  vs percent slant fracture



c. Steel

d. Normalized as  $Q_c/\sigma_{ys}$ Fig. 4 (Continued)—Crack extension force  $Q_c$  vs percent slant fracture

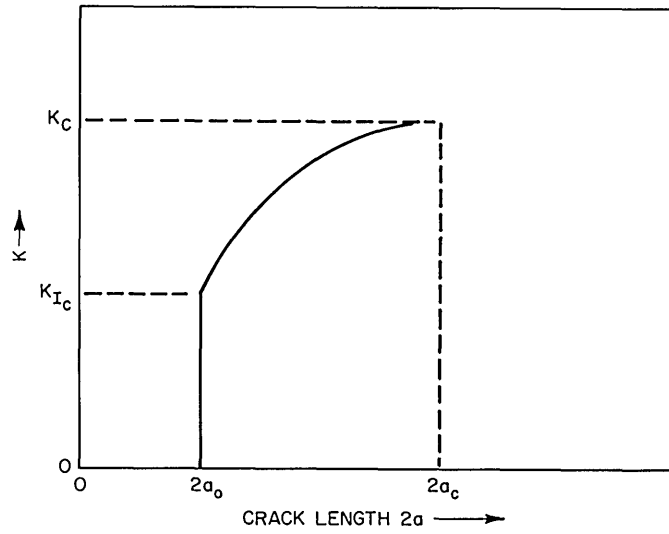


Fig. 5—Relationship of  $K_{Ic}$  and  $K_c$  to specimen crack length

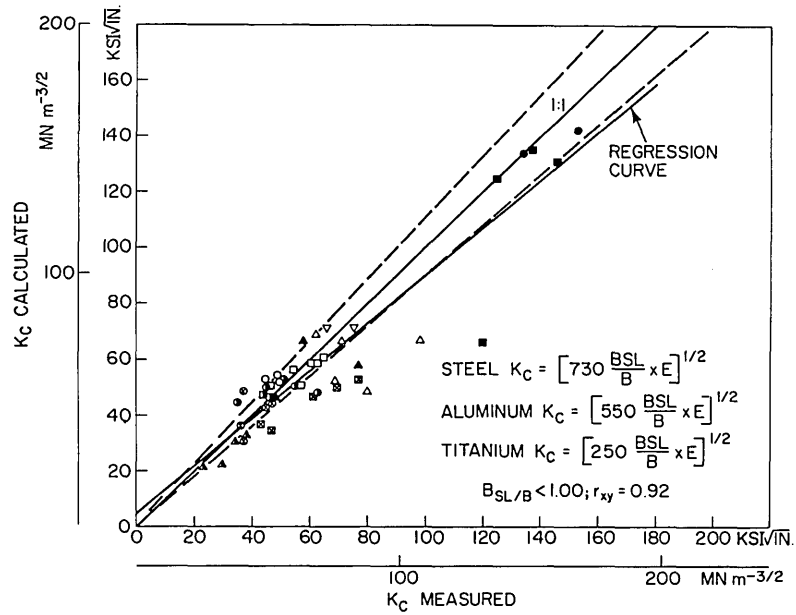


Fig. 6— $K_c$  calculated vs  $K_c$  measured for all alloys. Equations (3), (4), and (5) used for calculations.



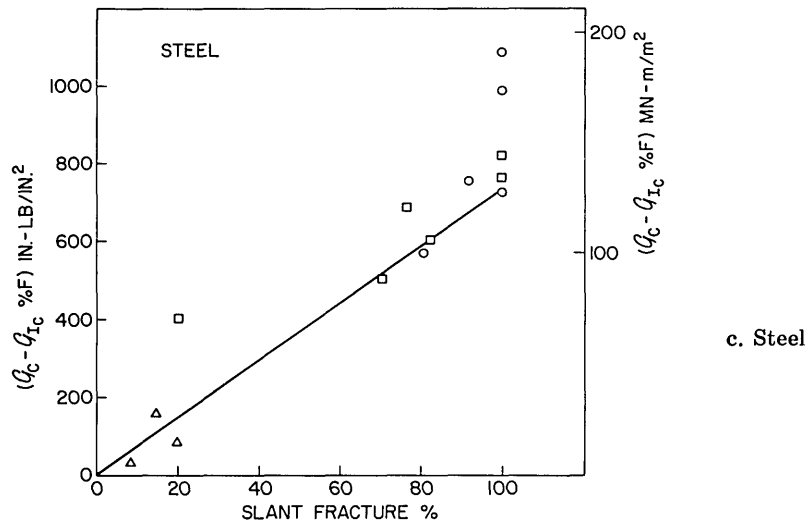
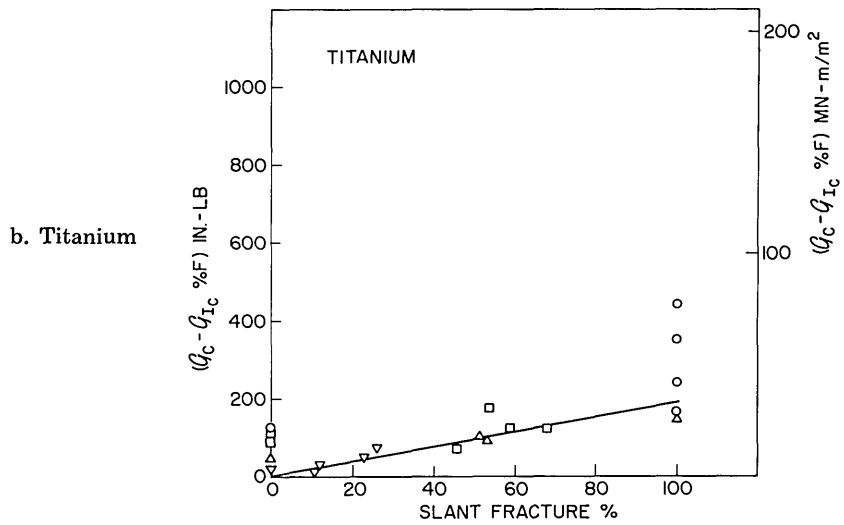
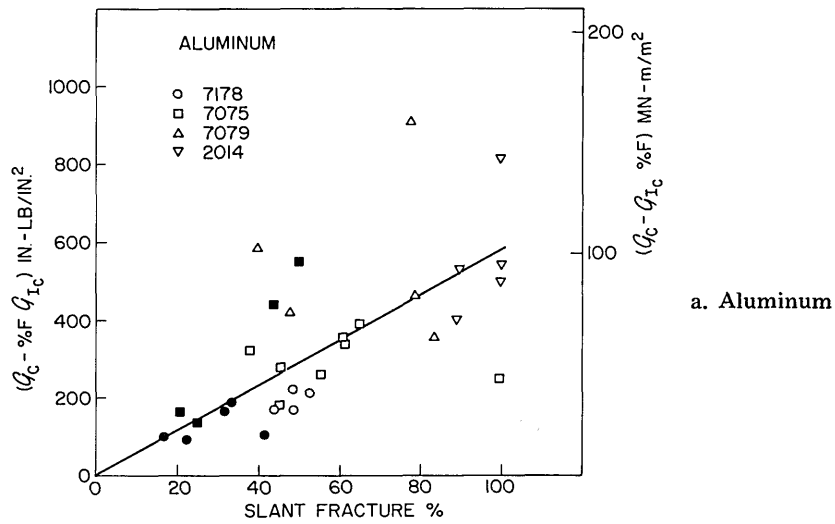


Fig. 7- $J_c^* [= J_c - J_{Ic}(B_F/B)]$  vs percent slant fracture

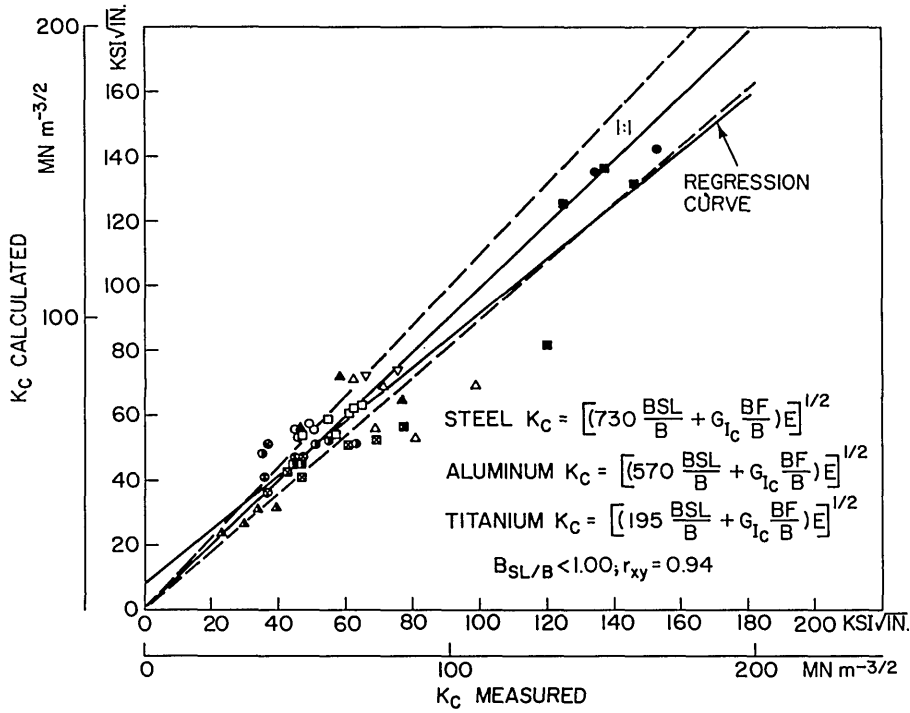


Fig. 8—Calculated  $K_c$  vs measured  $K_c$  for all alloys. Equations (8), (9), and (10) used for calculation.

$$\text{Steel } r_{xy} = 0.92$$

$$\text{Aluminum } r_{xy} = 0.63$$

$$\text{Titanium } r_{xy} = 0.76.$$

In view of the estimates involved, these values indicate definite correlations.

$\mathcal{J}_c$  values (here  $\mathcal{J}_c = \mathcal{J}_c^* + \mathcal{J}_{Ic}(B_F/B)$ ) were again calculated and converted to  $K_c$  values. For simplicity, Eqs. (8), (9), and (10) were employed for this purpose. The calculated and measured values are compared in Fig. 8. Statistical analyses of these data give a regression curve

$$K_c (\text{calc.}) = 0.84 K_c (\text{meas.}) + 8.2, \quad (14)$$

with a correlation coefficient of  $r_{xy} = 0.94$ .

The two models, I and II, earlier proposed consider the slant fracture contribution as a volume-sensitive mechanism. Model II suggests the relationship

$$\mathcal{J}_c = \mathcal{J}_c^{**} \frac{B_{SL0}^2}{B} + \mathcal{J}_{Ic} \frac{B_F}{B}, \quad (15)$$

where  $B_{SL0}$  = critical (constant) shear-lip thickness. Since a constant value for the amount of shear lip was rarely attained in the thickness series of alloys reported here, data for  $(\mathcal{J}_c - \mathcal{J}_{Ic})B_F/B$  against  $B_{SL}^2/B$  were computed and regression analyses determined. Values of the correlation coefficient for the three alloy systems are

|                   |         |
|-------------------|---------|
| Steel $r_{xy}$    | = 0.90  |
| Aluminum $r_{xy}$ | = 0.38  |
| Titanium $r_{xy}$ | = 0.53. |

From the relationships here developed,  $\mathcal{J}_c$  is seen constant for each given alloy system when  $B_{SL} < B$ . The ordering of the systems precludes normalization by either Young's modulus or density. Since the alloy systems also represent different crystallographic systems, it is suggested that these may influence the ordering, perhaps through the rolling textures developed. Clarification of this point might be assisted by investigations of fracture resistance in specimens with the fracture path transverse to the rolling direction ( $LT$ ).

## RELATIONSHIP BETWEEN INITIAL AND FINAL CRACK LENGTH

When a sheet specimen containing a notch is loaded in tension, the stress must reach a certain value before a crack will form at the notch tips. Once such a crack has initiated, it will grow under a rising load until the instability value is reached. Since computation of  $K_c$ , the fracture resistance value, requires knowledge of both stress and crack length at failure, crack length must be measured during the course of the test. A method for estimating the amount of crack extension from the initial notch length would be of practical value since it would eliminate the necessity for crack extension measurement. The question to be resolved is whether or not the final crack length  $2a_c$  is influenced by the initial crack length  $2a_0$ . Certain authors (21,22) have taken the position that no influence should exist, whereas others (23-26) indicate that an influence does exist. The results of this investigation suggest a form for a relationship between  $2a_c$  and  $2a_0$ .

When final crack length is plotted against initial crack length, a straight-line relationship can be observed. This is illustrated in Figs. 9a and b for aluminum alloy 7075-T6; other materials indicate a similar trend. Attempts to correlate this slope value with other parameters showed a relationship with the dimensionless value of

$$\beta_c = \left[ \frac{1}{B} \left( \frac{K_c}{\sigma_{ys}} \right)^2 \right].$$

Since the effect of thickness upon the value of  $K_c$  has been studied for a series of alloys, this information was analyzed.

Plotting the data on linear coordinate paper (Fig. 10) suggests the possibility of a linear-logarithmic relationship. Such a plot is seen in Fig. 11, together with the calculated regression curve and confidence limits.

For purposes of arithmetical expedience, the data were analyzed in the form

$$\ln 10 \left( \frac{a_0}{a_c} \right) = A + B \ln 10 \beta_c. \quad (16)$$

The regression curve calculated for 59 datum points is

$$\ln 10 \left( \frac{a_0}{a_c} \right) = 2.4367 - 0.1142 \ln 10 \beta_c, \quad (17)$$

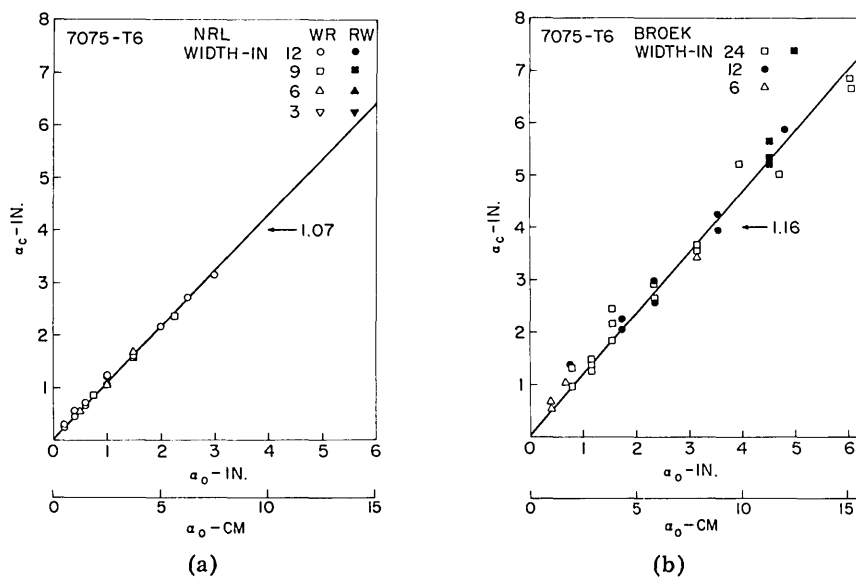


Fig. 9—Half critical crack length  $a_c$  vs half initial crack length  $a_0$

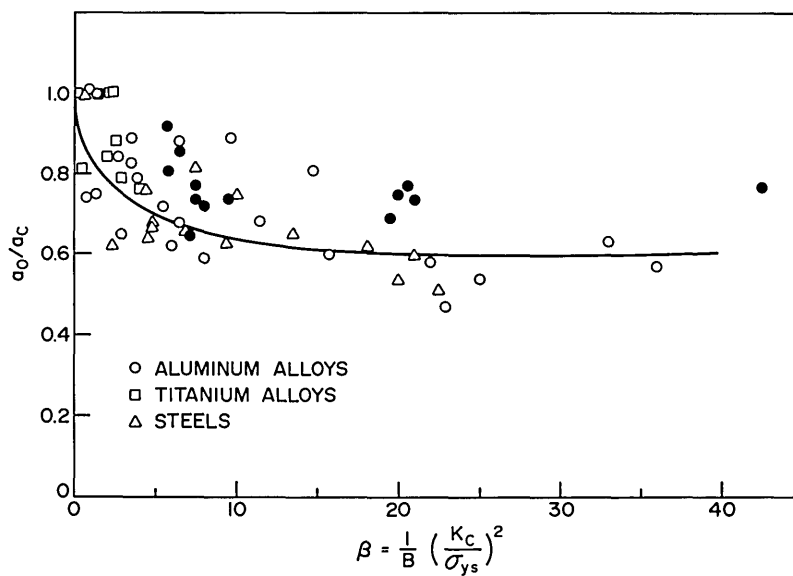


Fig. 10—Ratio of initial to critical crack length  $a_0/a_c$  vs  $\beta$ ;  $\beta = \frac{1}{B} \left( \frac{K_c}{\sigma_{ys}} \right)^2$

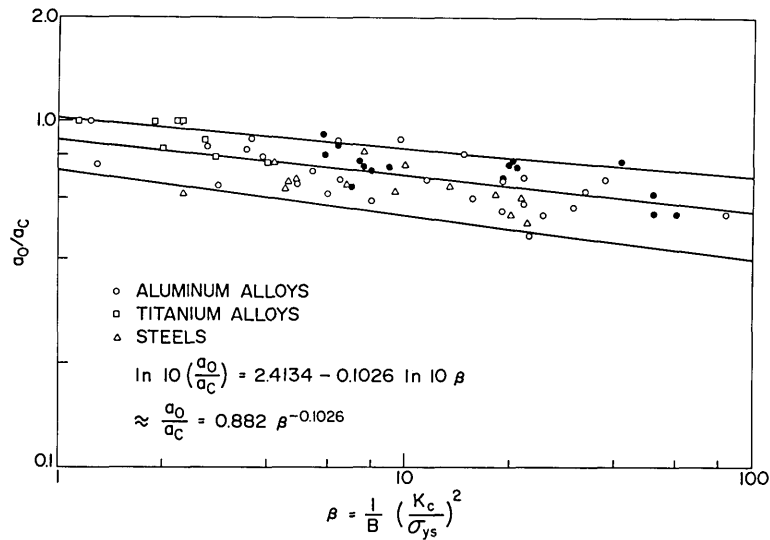


Fig. 11—Log  $a_0/a_c$  vs log  $\beta$ . Regression curve flanked by 95% confidence limit lines; closed symbols are for aluminum 7475-T61.

with a standard deviation for  $y = 0.21$  and a correlation coefficient  $r = 0.75$ . A  $t$ -statistic computed from the correlation coefficient equals  $-8.56$ , which is outside the 99% confidence interval of  $t = \pm 2.648$ ; this indicates that a relationship does exist between  $a_0/a_c$  and  $\beta$ .

Since the data comprised values obtained from testing aluminum, titanium and steel alloys, these data were also analyzed separately and intercompared. An analysis of variance ratios (F-statistic) indicates the following.

1. One regression line may be used for all three alloy systems;

$$F = 3.16 < F_{99\%} = 3.65.$$

2. The slopes of the three systems are equal;

$$F = 1.118 < F_{99\%} = 4.98.$$

3. Regression of the means is linear;

$$F = 6.53 < F_{99\%} = 7.08.$$

4. Slopes within groups are equal to the slope among groups;

$$F = 4.44 < F_{99\%} = 7.08.$$

Finally, another set of aluminum alloy data was added, bringing the number of datum points to 75. The regression curve computed is

$$\ln 10 \left( \frac{a_0}{a_c} \right) = 2.4134 - 0.1026 \ln 10 \beta_c, \quad (18)$$

with a standard deviation for  $\gamma = 0.20$  and a correlation coefficient  $r = 0.71$ . This equation was used to compute  $a_0/a_c$  for the last set of aluminum data (alloy 7475-T61) and  $K_c$  values from the estimates of  $2a_c$ . These estimates are included in Table 4. The fact that these are slightly high is rationalized by the fact that certain values of  $a_0/a_c = 1.00$  were included in the analysis. When no crack growth occurs with the sharp Elox notch tip, a fatigued crack might well have indicated slight growth and thus altered the constants in the regression curve. Nonetheless, it is believed that this analysis indicates the dependence of crack extension upon the initial crack and the feasibility of using such a relationship for estimation.

Because the final crack length  $2a_c$  employed for these analyses is the "effective" crack length determined from a COD calibration and includes a plastic zone factor, one might envision this relationship between initial and final crack length as indicating that the plastic zone size is influenced by some constraint factor in the specimen, since  $\beta = 2\pi r_y/B$ .

### SPECIMEN SCREENING

The relationship between  $K_c$  and  $\sigma_{ys}$  shown in Fig. 1 indicates the minimum specimen width required for various ratios of  $K_c/\sigma_{ys}$  (1). However, it is suggested that a width of 12 in. is adequate for the majority of high-strength materials.

The steps of a possible screening procedure are outlined below.

1. Estimate  $K_c$  from the relationship between  $K_c$  and  $\sigma_{ys}$  (Figs. 1 or 2).
2. Calculate  $\beta_c = \frac{1}{B} \left( \frac{K_c}{\sigma_{ys}} \right)^2$ .
3. Determine  $a_0/a_c$  from Fig. 11 and Eq. (18).
4. Select an initial crack length  $2a_0$  such that  $2a_c$  will be less than  $2a/W = 0.5$  (a generally acceptable crack length-to-width ratio is 0.3).
5. Perform the test; that is, load the specimen to fracture, recording the maximum load.
6. Compute  $K_c$  from the following equation:

$$K_c = \sigma_{G_{\max}} \sqrt{a_0 \left( \frac{a_c}{a_0} \right)} f \quad 2a/W. \quad (19)$$

### CONCLUSIONS

1. Degradation of  $K_c$  with increased yield stress is demonstrated by an inverse relationship.

2. Fracture resistance is directly related to the percent of slant fracture when  $B_{SL} < B$ , such  $\mathcal{J}_c^* = (\mathcal{J}_c - \mathcal{J}_{Ic}) B_F/B = A (B_{SL}/B)$ .

3. Values of the constant  $A$  for the different alloy systems suggest dependence upon the sheet rolling textures.

4. Final crack length at instability is influenced by the initial crack length.

5. The final crack length-initial crack length relationship is statistically acceptable in the form  $\ln 10 (a_0/a_c) = A - B \ln 10 \beta_c$  and can be transformed to  $a_0/a_c = A/\beta_c^B$ .

6. The relationship between  $a_0/a_c$  and  $\beta_c$  suggests that the plastic zone size varies with crack length.

7. Estimation of the final crack length permits a simplification of  $K_c$  determination for an initial screening test.

## ACKNOWLEDGMENT

The authors gratefully acknowledge the assistance of Dr. L. Wiener, Mathematics and Information Sciences Division, NRL, in providing consultation for and corroboration of the statistical analysis, and that of the Office of Naval Research for their financial support of these studies.

## REFERENCES

1. A.M. Sullivan, and C.N. Freed, "The Influence of Geometric Variables on  $K_c$  Values for Two Thin Sheet Aluminum Alloys," NRL Report 7270, June 17, 1971.
2. C.N. Freed, A.M. Sullivan, and J. Stoop, "Comparison of Plane-Stress Fracture Toughness for Three Aluminum Sheet Alloys," NRL Report 7299, Aug. 11, 1971.
3. A.M. Sullivan, and C.N. Freed, "Plane Stress Fracture Resistance of One Steel Sheet and Two Titanium Sheet Alloys," NRL Report 7332, Oct. 27, 1971.
4. C.N. Freed, A.M. Sullivan, and J. Stoop, "Crack-Growth Resistance Characteristics of High-Strength Sheet Alloys," NRL Report 7374, Jan. 31, 1972.
5. A.M. Sullivan, and C.N. Freed, "A Review of the Plane-Stress Fracture Mechanics Parameter  $K_c$  Determined Using the Center-Cracked Tension Specimen," NRL Report 7460, Dec. 29, 1972.
6. C.N. Freed, A.M. Sullivan, and J. Stoop, "Effect of Sheet Thickness on the Fracture Resistance  $K_c$  Parameter for Titanium Alloys," NRL Report 7464, Nov. 8, 1972.
7. A.M. Sullivan, and J. Stoop, "Effect of Sheet Thickness on the Fracture Resistance  $K_c$  Parameter for Steels," NRL Report 7601, Aug. 8, 1973.
8. C.N. Freed, A.M. Sullivan, and J. Stoop, "Influence of Dimensions of the Center-Cracked Tension Specimen on  $K_c$ ," ASTM STP 514, 1972, pp. 98-113.
9. A.M. Sullivan, C.N. Freed, and J. Stoop, "A Comparison of  $R$  Curves Determined from Different Specimen Types," ASTM STP 527, 1973.
10. A.M. Sullivan, J. Stoop, and C.N. Freed, "Plane Stress Fracture Resistance of High-Strength Titanium Alloy Sheet," *Titanium Science and Technology* (R.J. Jaffee and H.M. Burte, Eds.), New York, Plenum Press, 1973, *Proceedings, Second International Conference on Titanium, Boston, Mass., May 1971*.

11. A.M. Sullivan, J. Stoop, and C.N. Freed, "The Influence of Sheet Thickness Upon the Fracture Resistance of Structural Aluminum Alloys," *Progress in Crack Growth and Fracture Toughness Testing*, ASTM STP 536, 1973.
12. A.M. Sullivan, C.N. Freed, and J. Stoop, "Effect of Thickness Variations Upon the Plane Stress Fracture Resistance Parameter  $K_{Ic}$ ," *Proceedings of Third International Conference on Fracture, Munich, Germany, Apr. 1973*.
13. A.M. Sullivan and J. Stoop, "Further Aspects of Fracture Resistance Measurement on Thin Sheet Material: Yield Stress and Crack Length," presented at VII National Symposium on Fracture Mechanics, University of Maryland, Aug. 1973; ASTM STP (pending publication).
14. W.F. Brown, Jr., and J.E. Srawley, "Plane Strain Crack Toughness Testing of High-Strength Metallic Materials," ASTM STP 410, 1966.
15. C.C. Fretwell, "Regression Analysis," Program Library (300 Series) Vol. 1, 1968; Wang Laboratories, Tewkesbury, Mass.
16. B. Ostle, "Statistics in Research," Ames, Iowa, Iowa State University Press, 1963.
17. J.I. Bluhm, "A Model for the Effect of Thickness on Fracture Toughness," *Proc. ASTM*, 61, p. 1324 (1961).
18. J.M. Krafft, A.M. Sullivan, and R.W. Boyle, "Effect of Dimensions on Fast Fracture Instability of Notched Sheets," *Proceedings, Crack Propagation Symposium, College of Aeronautics, Cranfield, England, Vol. I, 1962*, pp. 8-28.
19. R.J. Goode and R.W. Judy, Jr., "Fracture-Safe Design of Aluminum and Titanium Alloy Structures," NRL Report 7281, Feb. 14, 1972.
20. W.S. Pellini, "Analytical Design Procedures for Metals of Elastic-Plastic and Plastic-Fracture Properties," *Welding Research Council Bulletin* 186, 1973.
21. C.M. Carman and G.R. Irwin, "Plane Stress Fracture Toughness Testing," Note for ASTM Committee E-24 Meeting, Cleveland, Ohio, October 1969.
22. D.Y. Wang, "Plane Stress Fracture Toughness and Fatigue Crack Propagation of Aluminum Alloy Wide Panels," *Progress in Crack Growth and Fracture Toughness Testing* ASTM STP 536, 1973.
23. F.C. Allen, "Stress Analysis of Centrally Cracked Plates," Douglas Paper 5513, presented to ASTM Committee E-24 on Fracture Testing, Philadelphia, Pa., March 1969.
24. D. Broek, "The Residual Strength of Light Alloy Sheets Containing Fatigue Cracks," *Aerospace Proceedings*, 1966, pp. 811-835.
25. R.G. Forman, "Experimental Program to Determine Effect of Crack Buckling and Specimen Dimensions on Fracture Toughness of Thin Sheet Materials," Air Force Flight Dynamics Laboratory Technical Report 65-146, January 1966.
26. J.C. Newman, Jr., "Fracture of Cracked Plates Under Plane Stress," *J. Engrg. Fracture Mech.* 1, 137-154 (1968).



## DOCUMENT CONTROL DATA - R &amp; D

(Security classification of title, body of abstract and indexing annotation must be entered when the overall report is classified)

|  |  |  |                       |
|--|--|--|-----------------------|
| 1. ORIGINATING ACTIVITY (Corporate author)<br>Naval Research Laboratory<br>Washington, D.C. 20375  |  | 2a. REPORT SECURITY CLASSIFICATION<br>Unclassified   |                       |
|  |  | 2b. GROUP  |                       |
| 3. REPORT TITLE<br><br>SOME FRACTURE MECHANICS RELATIONSHIPS FOR THIN SHEET MATERIALS  |  |  |                       |
| 4. DESCRIPTIVE NOTES (Type of report and inclusive dates)<br>Final report on one phase of a continuing NRL Problem.  |  |  |                       |
| 5. AUTHOR(S) (First name, middle initial, last name)<br><br>A.M. Sullivan and J. Stoop   |  |  |                       |
| 6. REPORT DATE<br>December 21, 1973  |  | 7a. TOTAL NO. OF PAGES<br>25   | 7b. NO. OF REFS<br>26 |
| 8a. CONTRACT OR GRANT NO.<br>NRL Problem M01-24  |  | 9a. ORIGINATOR'S REPORT NUMBER(S)<br><br>NRL Report 7650   |                       |
| b. PROJECT NO.<br>RR 022-01-46-5431  |  |  |                       |
| c.   |  | 9b. OTHER REPORT NO(S) (Any other numbers that may be assigned this report)                                    |                       |
| d.   |  |  |                       |
| 10. DISTRIBUTION STATEMENT<br><br>Approved for public release; distribution unlimited.   |  |  |                       |
| 11. SUPPLEMENTARY NOTES  |  | 12. SPONSORING MILITARY ACTIVITY<br>Department of the Navy<br>Office of Naval Research<br>Arlington, Va. 22217 |                       |
| 13. ABSTRACT<br><br>The fracture resistance parameter $K_c$ has been determined for a number of aluminum, titanium, and steel alloy sheet materials over a thickness range of 0.032 to 0.25 in. (0.8 to 6.25 mm). Several interesting $K_c$ relationships have been developed from these investigations.<br><br>The $K_c$ parameter is found to depend inversely upon the material yield stress. Further, a relationship can be established between $K_c$ and fracture appearance. Analysis of the data has also disclosed that the amount of crack extension, i.e., final crack length $2a_c$ appears to be influenced by the initial crack length. A straight-line curve in logarithmic coordinates relates the ratio of initial to final crack length, $a_0/a_c$ to $1/\beta_c$ ; this is justified by statistical analyses.<br><br>The development of these relationships can be of real assistance in the design of a standard initial screening test for $K_c$ . |  |  |                       |

| 14. KEY WORDS                      | LINK A |    | LINK B |    | LINK C |    |
|------------------------------------|--------|----|--------|----|--------|----|
|                                    | ROLE   | WT | ROLE   | WT | ROLE   | WT |
| Plane-stress fracture resistance   |        |    |        |    |        |    |
| Fracture mechanics parameter $K_c$ |        |    |        |    |        |    |
| Yield stress                       |        |    |        |    |        |    |
| Fracture appearance                |        |    |        |    |        |    |
| Slant or shear fracture            |        |    |        |    |        |    |
| Crack propagation                  |        |    |        |    |        |    |